

Vaccinia Virus Encodes I5, a Small Hydrophobic Virion Membrane Protein That Enhances Replication and Virulence in Mice[†]

Cindy L. Sood,¹ Jerrold M. Ward,² and Bernard Moss^{1*}

Laboratory of Viral Diseases¹ and Comparative Medicine Branch,² National Institute of Allergy and Infectious Diseases, National Institutes of Health, Bethesda, Maryland 20814

Received 27 June 2008/Accepted 3 August 2008

The vaccinia virus I5L open reading frame encodes a 79-amino-acid protein, with two predicted transmembrane domains, that is conserved among all sequenced members of the chordopoxvirus subfamily. No nonpoxvirus homologs or functional motifs have been recognized, and the role of the I5 protein remains unknown. We found that synthesis of I5 was dependent on viral DNA replication and occurred exclusively at late times, consistent with a consensus late promoter motif adjacent to the start of the open reading frame. I5 was present in preparations of purified virions and could be extracted with nonionic detergent, suggesting membrane insertion. Transmission electron microscopy of immunogold-labeled thawed cryosections of infected cells revealed the association of an epitope-tagged I5 with the membranes of immature and mature virions. Viable I5L deletion and frameshift mutants were constructed and found to replicate like wild-type virus in a variety of cell lines and primary human epidermal keratinocytes, indicating that the protein was dispensable for *in vitro* cultivation. However, mouse intranasal challenge experiments indicated that a mutant virus with a frameshift resulting in a stop codon near the N terminus of I5 was attenuated compared to control virus. The attenuation was correlated with clearance of mutant viruses from the respiratory tract and with less progression and earlier resolution of pathological changes. We suggest that I5 is involved in an aspect of host defense that is evolutionarily conserved although a role in cell tropism should also be considered.

The *Poxviridae*, a family of complex DNA viruses that replicate solely in the cytoplasm of their host cells, are comprised of the *Chordopoxvirinae* and the *Entomopoxvirinae* subfamilies (16). The orthopoxviruses, one of eight genera belonging to the chordopoxvirus subfamily, are the most intensively studied and best characterized poxviruses. Variola virus, a notorious member of this subfamily, has a host range that is restricted to humans and was the cause of smallpox until the disease was finally eradicated by immunization with vaccinia virus (VACV). The sequence similarity of many VACV and variola virus genes is greater than 90%, accounting for the immunological cross-reactivity and vaccine efficacy. VACV has been propagated for more than 200 years; it has become the laboratory prototype poxvirus and is widely employed as an expression vector (15). The original host of VACV is unknown although it is currently endemic in parts of Brazil (22), and a closely related virus has been isolated from Mongolian horses (23).

VACV has a linear double-stranded DNA genome with nearly 200 predicted open reading frames (ORFs). Only a few of the approximately 90 genes that are conserved in all chordopoxviruses (25) remain largely uncharacterized. One such protein, encoded by the I5L ORF, was identified as a component of the mature virion (MV) membrane by N-terminal sequencing of the fraction solubilized from purified MVs with NP-40 and 2-mercaptoethanol (21). The association of I5 (the

protein encoded by the I5L ORF) with sucrose gradient-purified MVs was corroborated by mass spectroscopy (2, 19, 26). Here, we show that I5 is expressed following viral DNA replication and is incorporated into the viral membrane at an early stage of morphogenesis. Despite its high conservation, I5 expression was not necessary or advantageous for virus replication and spread in a variety of cultured cells. Nevertheless, I5 was important for virus replication and virulence in a mouse model, suggesting a role in host interactions.

MATERIALS AND METHODS

Cells and viruses. BS-C-1 cells were maintained in minimum essential medium with Earle's salts supplemented with 2% fetal bovine serum, 100 units/ml of penicillin, and 100 µg/ml of streptomycin. HeLa cells were maintained in Dulbecco's modified Eagle's medium supplemented with 2% fetal bovine serum and antibiotics as described above. The VACV Western Reserve (WR) strain and recombinant viruses were propagated as previously described (6).

Antibodies. Rabbit antisera were raised against peptides derived from amino acids 38 to 52 (FTMQSLKFNRAVTIF) of the predicted I5 sequence and from amino acids 632 to 643 (QYISARHITELF) of the A3 sequence plus a C-terminal cysteine required for coupling to keyhole limpet hemocyanin (Covance Research Products, Princeton, NJ).

Plasmid and recombinant VACV construction. To construct the recombinant vΔI5GFP, the flanking regions of the I5L ORF were amplified from VACV strain WR genomic DNA template using oligonucleotides ct66 (5'-CAT CAT CCA TTA GAA TTT TCA ATT CCA CTA GCG TCA AAA AAT TTC CTA CT-3'), ct68 (5'-CAT AGA AAA AAA CAA AAT GAA ATT CTT ATA TCT AAA AAT TAG ATC AAA GAA T3-'), ct69 (5'-ATG GAC GAG CTG TAC AAG TAA CGT CAA ATC CCT ATT AAT GAA AA-3'), and ct71 (5'-TCA TAC AAC TAT TTT GGT TTT AAA ACT TTG GAA AAA TCC TAC TTG TTG AAA-3'). The ORF for enhanced green fluorescent protein (GFP) under VACV promoter p11 was amplified from pΔA43GFF (unpublished data) using primers ct67 (5'-ATT CTT TGA TCT AAT TTT TAG ATA TAA GAA TTT CAT TTT GTT TTT TTC TAT G-3') and ct70 (5'-TTT TCA TTA ATA GGG ATT TGA CGT TAC TTG TAC AGC TCG TCC AT-3'). Primers ct67 and ct68 as well as ct69 and ct70 were designed to complement each other. The above products were used in a second recombinant PCR to yield a GFP ORF flanked

* Corresponding author. Mailing address: Laboratory of Viral Diseases, National Institute of Allergy and Infectious Diseases, National Institutes of Health, 33 North Drive, MSC 3210, Bethesda, MD 20892-3210. Phone: (301) 496-9869. Fax: (301) 480-1535. E-mail: bmoss@nih.gov.

† Published ahead of print on 13 August 2008.

by regions up- and downstream of I5L. This construct preserved the last 28 nucleotides of the I5L ORF, which functions as a promoter for I4L. The resulting PCR product was gel purified and ligated into pCR-BluntII-Topo (Invitrogen, Carlsbad, CA), resulting in pΔI5GFP. The endogenous I5L ORF was replaced with the GFP marker gene by homologous recombination after transfection (Lipofectamine 2000; Invitrogen) of pΔI5GFP into VACV WR-infected cells. Recombinant viruses expressing GFP were detected with an inverted fluorescence microscope and isolated by three rounds of plaque purification. The correct site of recombination was verified by PCR analysis.

Recombinant vI5HA-GFP (where I5HA is I5 carrying a hemagglutinin [HA] epitope tag) was made in a similar manner as vΔI5GFP. The primers ct81 (5'-CAT ACG ATG TTC CAG ACT ACG CTT AAG AAT TTC ATT TTG TTT TTT TCT A-3') and ct71 were used to amplify GFP under the p11 promoter from vΔI5GFP, and primers ct82 (5'-TTC TTA AGC GTA GTC TGG AAC ATC GTA TGG GTA ACT TTT CAT TAA TAG GGA-3') and ct66 were used to amplify I5L from VACV strain WR genomic DNA template.

The I5 revertant virus (vI5Rev) and an I5 frameshift virus (vI5Stop) were derived from vΔI5GFP. Primers ct66 and ct71 were used to generate a PCR product containing the I5L gene including 500 bp of up- and downstream sequence. The resulting PCR product was gel purified and ligated into pCR-BluntII-Topo, resulting in pI5Rev. Homologous recombination was used to replace the GFP marker gene with the endogenous I5L ORF after transfection of pI5Rev into cells infected with vΔI5GFP. Non-GFP-expressing plaques were picked and isolated by three rounds of plaque purification. The correct site of recombination was verified by PCR and sequence analysis. A stop codon was generated in the I5L sequence of pI5Rev by using a QuickChange site-directed mutagenesis kit (Stratagene, La Jolla, CA) with PCR oligonucleotides containing the desired mutation. Primers ct91 (5'-GCA TAA CTG TAT TAA TGC TTT TGA TGT AAT TTC TGG TGC CGC CCT G-3') and ct92 (5'-CAG GGC GGC ACC AGA AAT TAC ATC AAA AGC ATT AAT ACA GTT ATG C-3') were used to delete nucleotide 61, resulting in an immediate stop codon. Homologous recombination was used to replace the GFP marker gene with the I5Stop sequence after transfection of pI5Stop into vΔI5GFP-infected cells. Again, non-GFP-expressing plaques were picked and isolated by three rounds of plaque purification. The correct site of recombination was verified by PCR and sequence analysis.

SDS-PAGE. Cells were lysed in 0.2% NP-40 (10 mM Tris, pH 7.4, 10 mM CaCl₂, 10 mM NaCl) containing 8 µg/ml micrococcal nuclease (Worthington Biochemical Corp., Lakewood, NJ) at 4°C for 20 min. After addition of lithium dodecyl sulfate sample buffer and reducing agent (Invitrogen, Carlsbad, CA), cell lysates were heated to 70°C for 10 min. Equal volumes of lysate were analyzed by sodium dodecyl sulfate-polyacrylamide gel electrophoresis (SDS-PAGE) on a 10% bis-Tris-MES [2-(N-morpholino)ethanesulfonic acid]-SDS running buffer (Invitrogen).

Western blot analysis. Proteins separated by SDS-PAGE were electrophoretically transferred to polyvinylidene difluoride membrane (Invitrogen). Membranes were blocked in Tris-buffered saline with 5% nonfat dry milk and 0.05% Tween 20 and then incubated with antibodies for 1 h at room temperature or overnight at 4°C. Protein bands were visualized by chemiluminescence using West-Pico or Dura kits (Pierce Biotechnology Inc., Rockford, IL).

Analysis of virion extracts. VACV MVs, purified by two sucrose cushions and one sucrose gradient centrifugation from cells infected with vI5HA-GFP, were incubated at 37°C for 1 h in 50 mM Tris (pH 7.4) or in 1% NP-40 in 50 mM Tris (pH 7.4) in the presence or absence of 50 mM dithiothreitol (DTT). Soluble and insoluble fractions were separated by centrifugation at 30,000 × g for 30 min and resuspended to equal volumes in sample buffer containing lithium dodecyl sulfate. Equivalent amounts of each fraction were loaded on a 10% polyacrylamide gel and subjected to electrophoresis. The separated proteins were transferred to a polyvinylidene difluoride membrane and analyzed by Western blotting as described above.

Confocal microscopy. HeLa cells were grown on glass coverslips in 12-well plates. Cells were infected at multiplicity of 0.5 PFU per cell. At 24 h postinfection, cells were fixed with 4% paraformaldehyde in phosphate-buffered saline (PBS) for 7 min at room temperature, washed three times with PBS, and then permeabilized for 10 min with 0.1% Triton X-100 in PBS at room temperature. Cells were blocked for 1 h with 10% fetal bovine serum in PBS, followed by incubation with primary antibody at room temperature. Cells were washed three times in PBS, followed by incubation with Alexa Fluor 594-conjugated secondary antibody (Invitrogen) at room temperature. After cells were washed three times with PBS, DNA was stained with 4'-6'-diamidino-2-phenylindole (DAPI), and coverslips were mounted on slides with Mowiol. Images were collected with a Leica TCS-NT/SP2 inverted confocal microscope system.

Electron microscopy. BS-C-1 cells were grown in dishes of 60-mm diameter and infected with 5 PFU of virus per cell for 20 h. Cells were prepared for conventional transmission electron microscopy by fixing with 2% glutaraldehyde and embedding in EmBed-182 resin (Electron Microscopy Sciences, Hatfield, PA). Alternatively, cells were fixed with 4% paraformaldehyde–0.05% glutaraldehyde in 0.1 M phosphate buffer for 1 h at room temperature and incubated in 10% gelatin at 37°C. The cell pellet was collected by centrifugation, solidified on ice, cut at 4°C into small cubes infiltrated with 2.3 M sucrose in 0.1 M phosphate buffer, frozen on pins in liquid nitrogen, and cut into 70-nm sections on a Leica Ultracut FCS microtome (Wetzlar, Germany). Cryosections were picked up on grids, thawed, washed free of sucrose, and stained with a monoclonal antibody to a HA epitope tag (Invitrogen) followed by rabbit anti-mouse immunoglobulin G (IgG) and protein A conjugated to 10-nm gold spheres. Specimens were viewed with an FEI-CM100 transmission electron microscope (Hillsboro, OR).

Determination of virulence in mice. Female BALB/c mice were purchased from Taconic (Germantown, NY) and maintained in a pathogen-free environment in sterile microisolator cages. Groups (*n* = 10) of 7-week-old mice were anesthetized by inhalation of isoflurane and inoculated via the intranasal (i.n.) route with a 20-µl suspension of purified VACV into one nostril. Mice were weighed daily for 2 weeks following challenge and were euthanized when they lost 30% of their initial body weight, according to a protocol approved by the National Institute of Allergy and Infectious Diseases Animal Care and Use Committee. Inoculum titers were determined in order to confirm the dose administered.

Titration of virus from lung. Lungs were removed from mice that had been infected i.n. with 1 × 10⁴ PFU of vI5Stop or vI5Rev; lungs were placed in 2 ml of PBS with 0.05% bovine serum albumin and kept at -80°C until use. Lungs were thawed and ground until a uniform homogenate was formed, frozen and thawed three times, and sonicated three times for 30 s. Viral titers were determined by plaque assay on BS-C-1 cells.

Histological analysis. A total of 17 mice were infected i.n. with 1 × 10⁴ PFU of vI5Stop or vI5Rev and necropsied on days 3, 5, 7, and 10. Lungs were inflated with 10% neutral buffered formalin, and other tissues were also fixed in formalin and embedded in paraffin, and sections were stained with hematoxylin and eosin. Whole lung sections were prepared from each mouse. Histopathological changes in the nasal cavity were graded in a random, blinded fashion as to extent of tissue involvement and severity, with grades of 1 to 4 as indicated in the legend of Fig. 10. For immunohistochemistry, a rabbit polyclonal antibody (4) was used at 1:2,000, followed by the Mach 4 horseradish peroxidase polymer (Biocare Medical, Concord, CA) and diaminobenzidine.

RESULTS

Conservation of the I5L ORF in chordopoxviruses. The I5L ORF (VACV WR074) is predicted to encode a 79-amino-acid protein lacking cysteine, histidine, and tryptophan residues with a mass of approximately 8.7 kDa. A hydrophilicity plot showed two putative transmembrane domains with very short N- and C-terminal sequences and only 18 amino acids between the two helices (Fig. 1A). The N-terminal sequence data of Takahashi and coworkers (21) indicated the absence of a cleavable signal peptide. No nonpoxvirus homologs were found, nor were any functional sequence motifs predicted. However, all chordopoxvirus genomes sequenced to date contain an I5L ortholog (www.poxvirus.org). The amino acid sequence identities between I5 orthologs range from 94 to 100% among orthopoxviruses and 30 to 49% between members of different genera (Fig. 1B).

The I5 protein is synthesized at late times during VACV infection and incorporated into virions. In order to specifically detect the I5 protein with antibody, we constructed a recombinant virus with an influenza virus HA epitope tag at the C terminus of I5 without modifying the promoter, which contains a late consensus TAAATG motif (5). To facilitate the isolation of the recombinant virus, we also inserted an ORF encoding GFP regulated by the VACV late p11 promoter between the I5 and I4 ORFs. The resulting virus, vI5HA-GFP, formed nor-

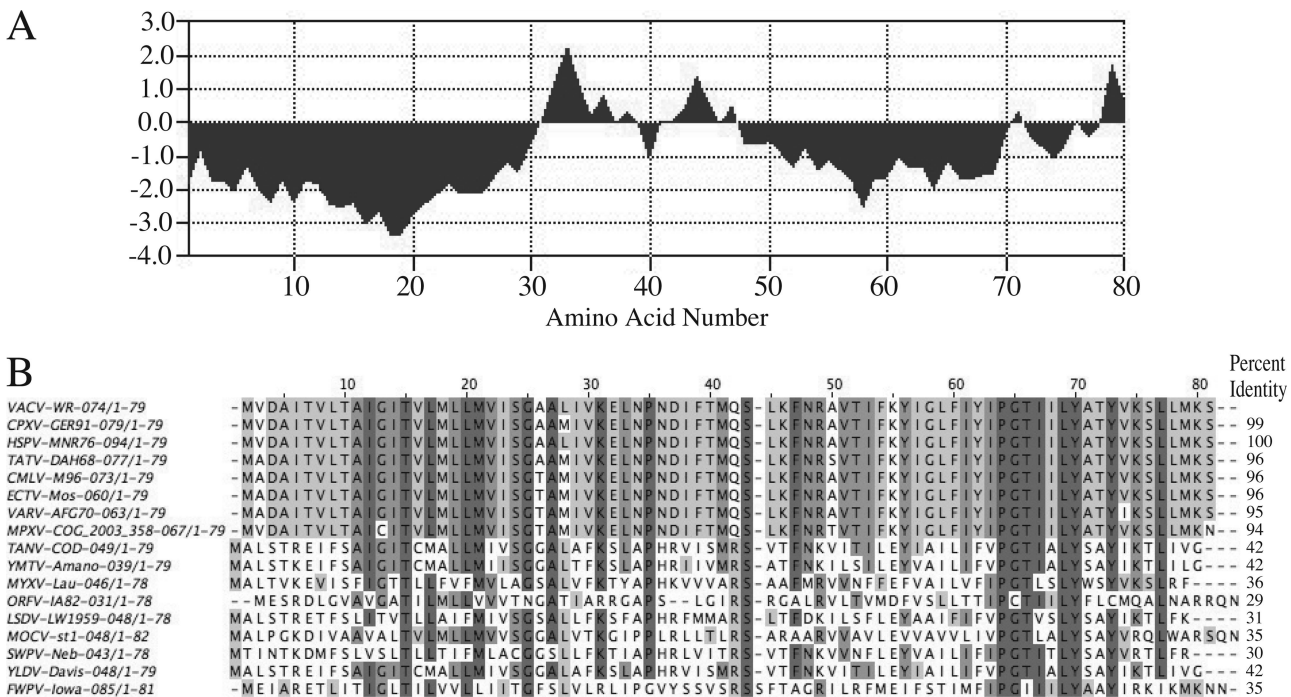


FIG. 1. Hydrophilicity of I5 and multiple sequence alignment of orthologs. (A) Hydrophilicity plot (9) of VACV I5. (B) A multiple sequence alignment was constructed using Jalview (3). Sequences from eight orthopoxvirus species and one or more representatives of other chordopoxvirus genera were included in the alignment. Shading increases with the degree of amino acid conservation. The percent identities between VACV WR074 and orthologs are listed on the right. Abbreviations: CPXV, cowpox virus; HSPV, horsepox virus; TATV, taterapox virus; CMLV, camelpox virus; ECTV, ectromelia virus; VARV, variola virus; MPXV monkeypox virus; TANV, tanapox virus; YMTV, yaba monkey tumor virus; ORFV, orf virus; LSCV, lumpy skin disease virus; MOCV, molluscum contagiosum virus; SWPV, swinepox virus; YLDV, yaba-like disease virus; FWPV, fowlpox virus.

mal-size green plaques when viewed by fluorescence microscopy. At sequential times postinfection with vI5HA-GFP, whole-cell extracts were analyzed by SDS-PAGE. The proteins were blotted to a membrane and probed with an antibody to the HA epitope tag. At 6 h after infection, a band that migrated with an estimated mass of approximately 9 kDa was detected. This band was increased in intensity from 8 to 24 h (Fig. 2A). A similar time course was found for the product of the A3L ORF (Fig. 2A), a well-characterized late protein that appears as a doublet because of proteolytic processing (8). Neither I5HA nor A3 was detected when cells were infected in the presence of cytosine arabinoside (not shown), indicating a requirement for viral DNA replication that was consistent with late stage expression.

MVs were purified by sucrose gradient sedimentation from cells infected with vI5HA-GFP, and the presence of I5HA was demonstrated by Western blotting with antibody to the epitope tag. I5HA was mostly extracted with 1% NP-40 and completely solubilized when DTT was added, similar to the well-characterized L1 MV membrane protein (Fig. 2B). This result supported previous data indicating that I5 is a component of the MV membrane.

Localization of I5 to viral factories and assembling virions.

Localization of I5 to viral factories and assembling virions. Confocal microscopy was performed to determine whether I5 associates with cellular membranes in addition to virions. Following infection with vI5HA-GFP, cells were fixed, permeabilized, and stained with antibody to the HA tag, followed by a fluorescently labeled secondary antibody. Cytoplasmic facto-

ries, the site of viral DNA replication and virion assembly, were visualized by staining with DAPI, which forms fluorescent complexes with double-stranded DNA. At late times after infection, factories may appear pleomorphic but are typically located adjacent to the nucleus, which also stains with DAPI. The I5 protein colocalized with viral factories (Fig. 3), consistent with incorporation into virus particles. As a control, no specific antibody staining was found when cells were infected with an I5L deletion mutant ($v\Delta I5GFP$) to be described below (Fig. 3).

Further experiments were carried out to determine the developmental stage at which I5 associates with viral membranes. Thawed cryosections of cells infected with vI5HA-GFP were stained with antibody to HA, followed successively by a secondary antibody and gold spheres conjugated to protein A. The grids were then examined by transmission electron microscopy. Gold grains were associated with immature virions and MVs as well as later-stage wrapped forms and extracellular enveloped virions (Fig. 4). Many of the gold spheres were on or close to the viral membrane, though some seemed to be more internal. An internal appearance can result from surface immunostaining of wedge-shaped sections (20).

I5 is nonessential for virus replication in cultured cells. In view of the conservation of I5, we suspected that the gene would be essential for virus replication. To confirm or refute this expectation, we transfected a plasmid containing the GFP ORF regulated by a late promoter between I5L flanking sequences into cells infected with VACV WR. An inability to

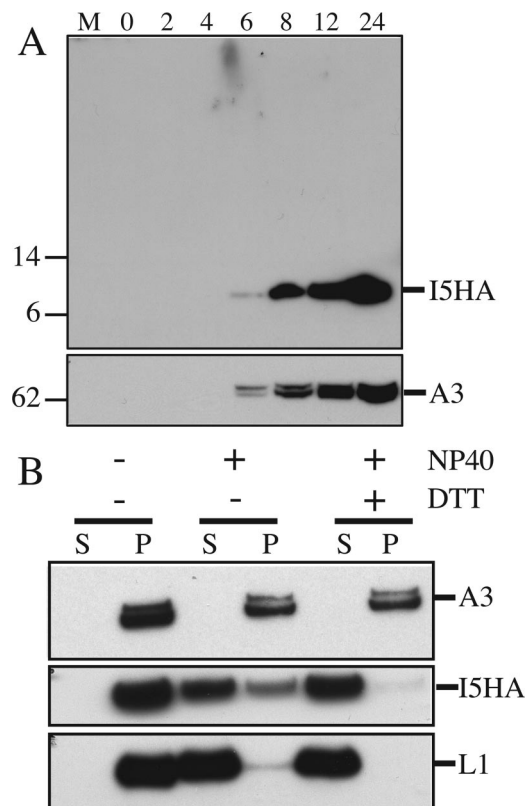


FIG. 2. Synthesis of I5 and MV membrane localization. (A) I5 expression kinetics. BS-C-1 cells were infected with vI5HA-GFP at a multiplicity of 15 PFU per cell. At the indicated hours postinfection, cell extracts were prepared and analyzed by SDS-PAGE and Western blotting with antibody to the HA epitope tag. Masses (in kDa) of marker proteins are on the left. The blot was stripped and reprobed with antibody to the A3 protein, which appears as a doublet due to processing during virus maturation. M, mock infected. (B) Extraction of I5 from MVs. Sucrose gradient-purified vI5HA-GFP MVs were treated with NP-40 or NP-40 and DTT or mock treated and separated into soluble (S) and pellet (P) fractions. Proteins in both fractions were resolved by SDS-PAGE, followed by Western blotting with antibody to HA, A3, or L1 as indicated.

isolate green fluorescent plaques would suggest that a deletion mutant was not viable. However, green plaques were readily isolated on BS-C-1 cells, and deletion of the I5L ORF was confirmed by PCR. Further characterization indicated no appreciable difference in plaques formed by vΔI5GFP and VACV WR on BSC1, BHK, CV-1, HeLa, HuTK⁻, and RK13 cells and on primary human epidermal keratinocytes, indicating normal virus replication and spread (data not shown). Moreover, the yields of vΔI5GFP and VACV WR in BS-C-1 cells were similar (data not shown). In addition, the morphologies of cells infected with the deletion mutant and wild-type virus were similar, without signs of nuclear fragmentation or cytoplasmic blebbing.

Depending on the site of insertion, expression of GFP from a strong promoter can have subtle effects on virus replication, and this is particularly important if *in vivo* studies are planned. Therefore, we derived two additional viruses. Homologous recombination was used to replace the GFP ORF of vΔI5GFP with either the wild-type I5L ORF to generate the control vI5Rev or with the I5L ORF containing a deletion of nucleotide 61, resulting in an immediate stop codon, to generate vI5Stop. In both cases recombinant virus plaques were recognized by the absence of green fluorescence and clonally purified. PCR and DNA sequencing confirmed the expected genome alterations. As expected, I5 could not be detected by Western blotting of lysates of cells infected with either vΔI5GFP or vI5Stop, indicating premature translational termination in the latter case (Fig. 5C). The plaque sizes and virus yields of vI5Stop and vI5Rev were indistinguishable (Fig. 5A and B). Furthermore, all stages of morphogenesis appeared normal as determined by transmission electron microscopy (Fig. 6).

I5 contributes to virulence in mice. The conservation of I5 suggested an important function despite the ability of vΔI5GFP and vI5Stop to replicate in cultured cells. We therefore considered the possibility that I5 has a role in host interactions that might be discerned only *in vivo*. An i.n. mouse model of infection (24) was used to determine if expression of

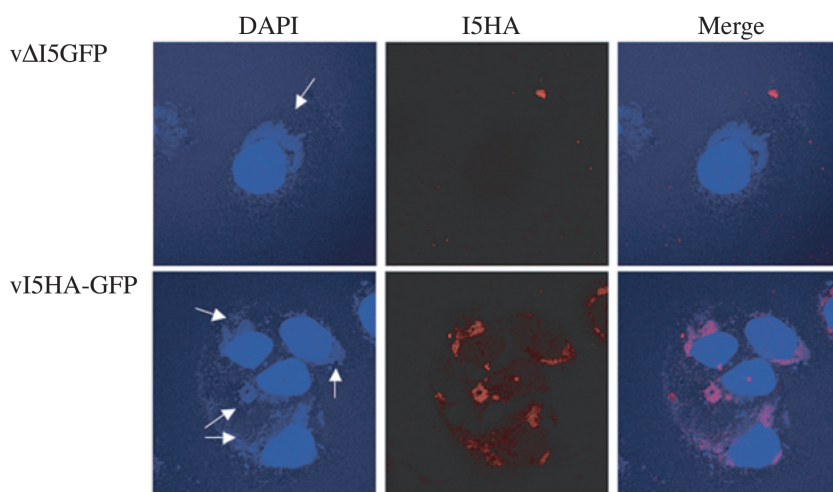


FIG. 3. Localization of I5 in cytoplasmic viral factories. HeLa cells were infected with vI5HA-GFP or vΔI5GFP at a multiplicity of 0.5 PFU per cell. After 24 h, cells were fixed, permeabilized, and stained with anti-HA monoclonal antibody, followed by Alexa Fluor 594-conjugated anti-mouse antibody (red). DNA was stained with DAPI (blue). Images were viewed by confocal microscopy. Arrows indicate viral factories.

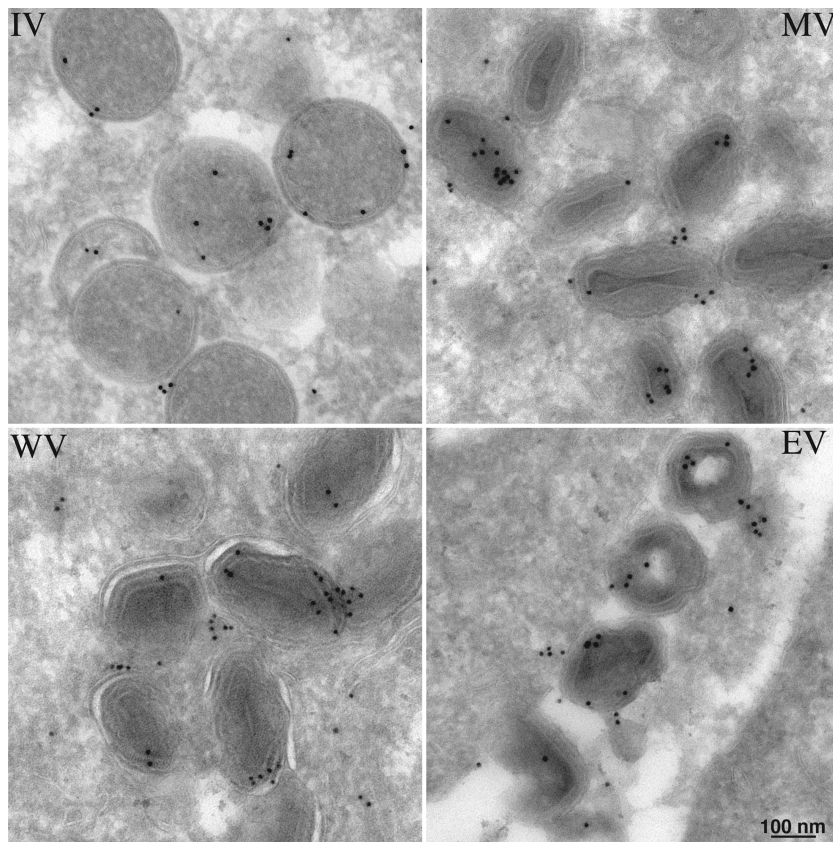


FIG. 4. Immunogold labeling of I5 associated with immature virions and MVs. BS-C-1 cells were infected with vI5HA-GFP at a multiplicity of 5 PFU per cell. After 18 h, the cells were fixed and frozen. Thawed cryosections were incubated with mouse monoclonal antibody to HA, rabbit IgG to mouse IgG, and then with 10-nm diameter gold particles conjugated to protein A. Electron microscopic images are shown with a 100-nm scale bar. IV, immature virions; WV, wrapped virions; EV, enveloped virions.

I5 is important for virulence. Groups of 10 mice received 10^4 , 10^5 , or 10^6 PFU of vI5Rev or vI5Stop i.n. under anesthesia. Weight change and survival were recorded daily and compared to an uninfected control group. All mice that received 1×10^4

PFU of vI5Stop survived and exhibited less severe weight loss ($P = 0.0003$, day 7; Mann Whitney test) than mice that received the same amount of vI5Rev (Fig. 7). More decisively, mice that received 1×10^5 PFU of vI5Stop had a 90% survival rate while mice that received 1×10^5 PFU of vI5Rev had a 0% survival rate (Fig. 7A). However, with a challenge dose of 1×10^6 PFU, there were no survivors in any of the groups (data not

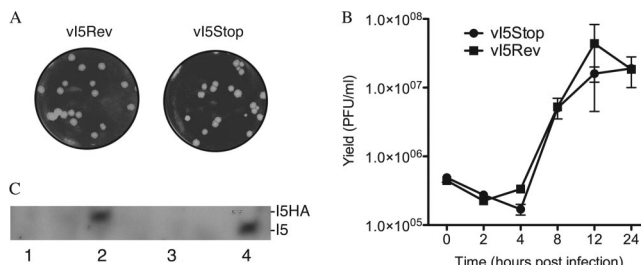


FIG. 5. Comparison of vI5Stop and vI5Rev replication. (A) Plaque phenotypes of vI5Rev and vI5Stop. Monolayers of BS-C-1 cells were infected with vI5Rev or vI5Stop. After 48 h, cells were fixed and stained with crystal violet. (B) One-step growth curves of vI5Rev and vI5Stop. BS-C-1 cells were infected with vI5Rev or vI5Stop at a multiplicity of 10 PFU per cell. Virus yields were determined from 2 to 24 h postinfection by plaque assay. (C) Western blots. Proteins in lysates of cells that were infected with vI5GFP (lane 1), vI5HA-GFP (lane 2), vI5Stop (lane 3), or vI5Rev (lane 4) were resolved by SDS-PAGE and analyzed by Western blotting with rabbit polyclonal antibody to I5. The bars indicate the positions of I5HA and unmodified I5.

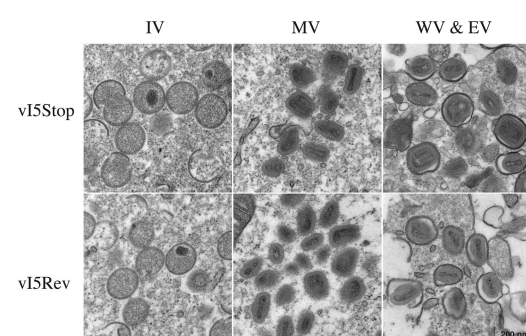


FIG. 6. Transmission electron microscopy of cells infected with vI5Stop and vI5Rev. BS-C-1 cells were infected with vI5Stop or vI5Rev at a multiplicity of 5 PFU per cell. At 20 h after infection, the cells were fixed and prepared for electron microscopy. Electron microscopic images are shown with a 200-nm scale bar. IV, immature virions; WV, wrapped virions; EV, enveloped virions.

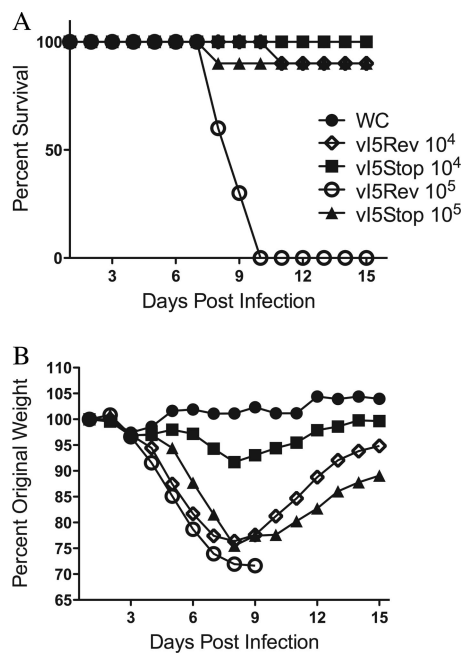


FIG. 7. Virulence of vi5Stop and vi5Rev in mouse i.n. infection model. Groups of 10 BALB/c mice were inoculated intranasally with 10^4 , 10^5 , or 10^6 PFU of purified vi5Stop or vi5Rev. (A) Percent survival of mice. (B) Percentage of original weight of mice. WC, untreated and uninfected weight control. Symbols in panels A and B are the same.

shown). Thus, I5 is important for virulence although vi5Stop was still lethal at a high dose.

I5 enhances VACV replication in the lung. Previous studies have shown that high titers of VACV WR occur in the lungs following i.n. inoculation and that this correlates with morbidity and death (10, 11, 13, 18). In order to compare the spread of vi5Stop and vi5Rev in the lower respiratory tract, we inoculated a sublethal dose of 1×10^4 PFU of vi5Stop and vi5Rev i.n. and quantified viral titers in the lungs on days 3, 5, and 7. The titers of vi5Rev and vi5Stop on day 3 were similar, suggesting that I5 was not required to establish an initial infection (Fig. 8A). However, on day 5 the amount of vi5Stop began to decline, whereas the amount of vi5Rev increased (Fig. 8A). This trend continued on day 7, indicating that the vi5Stop virus was cleared rapidly. To confirm these results, the experiment was repeated with a large number of mice ($n = 10$) in each group, and the day 7 lung titers were determined. Although the weights of the lungs from the mice infected with vi5Stop were slightly higher than those of vi5Rev, the virus lung titers were significantly lower ($P = 0.0002$) (Fig. 8B). These results confirmed the lower progression and more rapid clearance of vi5Stop from the host.

Pathology induced by vi5Stop and vi5Rev. Mice were infected i.n. with 1×10^4 PFU of vi5Stop or vi5Rev as described in the preceding section. Upper and lower respiratory tract tissue sections were examined by staining with hematoxylin and eosin and antibodies to VACV in order to discern differences in virulence. Both viruses infected the nasal epithelium and underlying glandular tissues. Destruction of the nasal epithelium occurred without inducing much of an inflammatory infiltrate. However, the lesions produced by vi5Stop were less

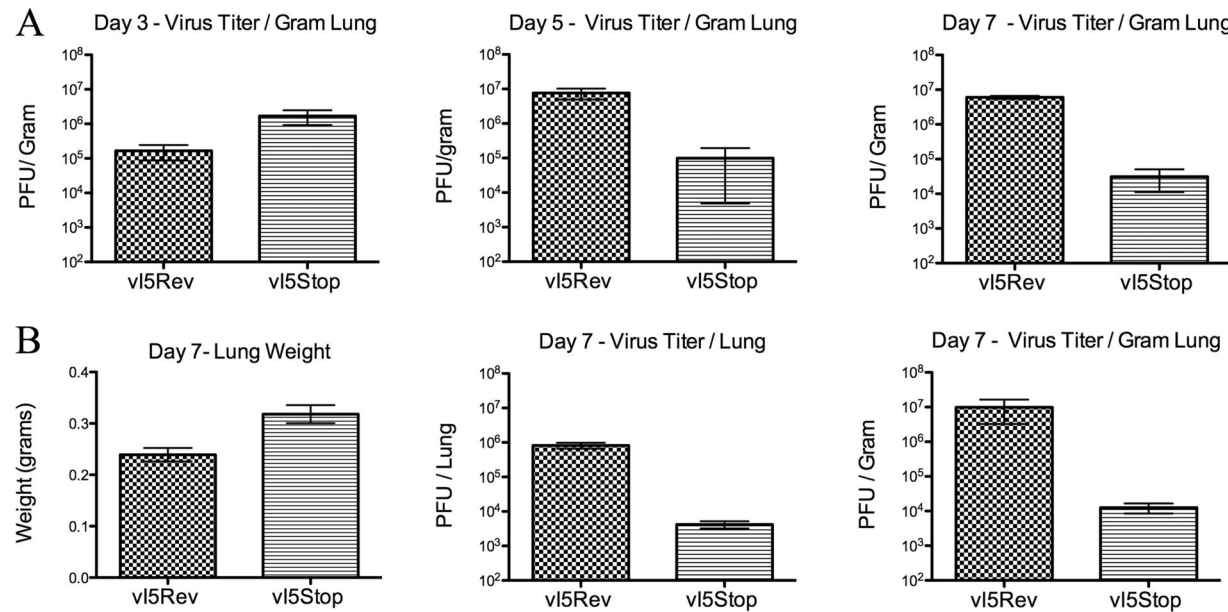


FIG. 8. Virus titers in the lungs of infected mice. BALB/c mice were inoculated i.n. with 1×10^4 PFU of purified vi5Stop or vi5Rev. Lungs were excised, weighed, and then titers were determined by plaque assay to determine virus load. (A) Viral titers per gram of lung tissue obtained on days 3, 5, and 7. Titers were determined on lungs from three mice infected with each virus, and standard errors of the mean are indicated. (B) Lung weights and viral titers on day 7. Lung weights, viral titer/lung, and viral titer/gram of lung are plotted. Titers were determined on lungs from 10 mice infected with each virus, and standard errors of the mean are shown. A Mann Whitney t test yielded a P value of 0.005 in a comparison of the lung weights from mice infected with the two viruses and a P value of 0.0002 in a comparison of the viral titer/gram of lung from the two viruses.

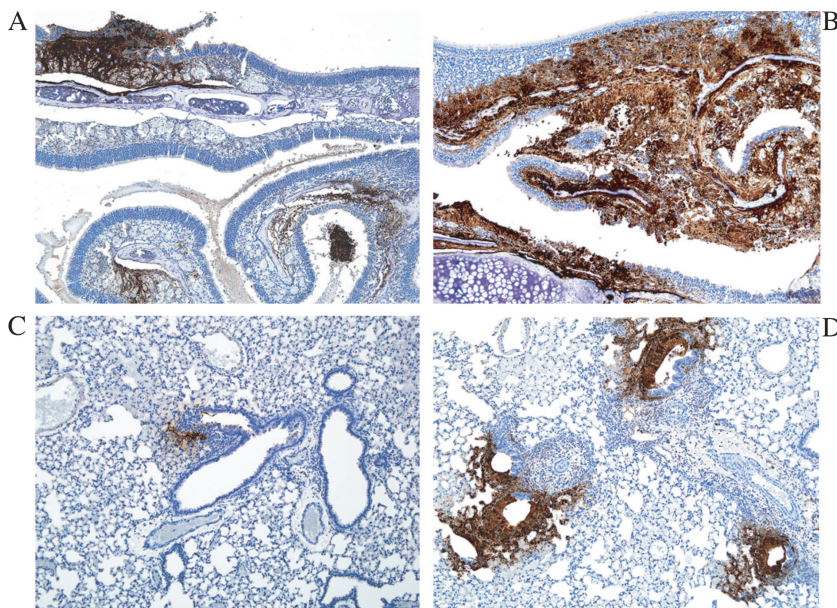


FIG. 9. Immunostained sections of nasal epithelium and lung from infected mice. Mice were infected i.n. with 1×10^4 PFU of vi5Stop or vi5Rev. Nasal sections and lung tissue were fixed in formalin and paraffin embedded. Histochemistry was performed with an antibody to VACV proteins. Images are at a magnification of $\times 100$. (A) Nasal epithelium infected with vi5Stop at day 7. Note the focus of infection stained brown. (B) Nasal epithelium infected with vi5Rev at day 7. Note the extent of the lesions and abundant antigen. (C) Lung infected with vi5Stop at day 5 showing one bronchiole infected with associated necrosis and inflammation. (D) Lung infected with vi5Rev at day 5 showing three bronchioles infected.

severe and more focal than those caused by vi5Rev (Fig. 9A and B). Furthermore, the severity and extent of the lesions produced by vi5Stop decreased after day 7 whereas those produced by vi5Rev continued to increase (Fig. 10). With both viruses, infection of the lungs occurred focally in the bronchiolar epithelial cells and around bronchioles. The lesions and viral infection appeared less severe in the mice receiving vi5Stop than in vi5Rev-infected mice, and in both cases the pathology was less extensive than in the nasal cavities (Fig. 9C and D).

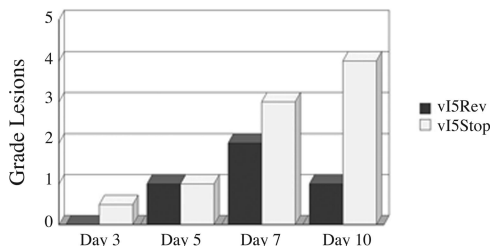


FIG. 10. Graded lesions of nasal epithelium on indicated days after infection with vi5Stop and vi5Rev. Two to three sections of the nasal cavity (including the squamous, respiratory, and olfactory regions of the epithelium) from each of the 17 mice in this study were stained with antibody to vaccinia virus. The entire slide was scanned to make a virtual computerized slide and a section representing average antigen expression for each mouse was selected. After an initial examination, grading was done in a random blinded fashion as follows: 0, no stained foci seen; 1, few positive focal areas; 2 several positive foci or large positive areas; 3, many positive foci or larger positive areas; 4, numerous coalescing positive areas.

DISCUSSION

We have provided the first detailed characterization of the product of the I5L gene of VACV. Although previous studies had suggested that I5 is a component of the MV membrane (21), its function was not predicted because of the absence of any recognizable functional motif or nonpoxvirus homolog. We confirmed the association of I5 with the MV membrane by biochemical and electron microscopic methods. Expression of I5 was dependent on viral DNA replication, and the protein was associated with the membranes of both immature and mature virions in viral factories. I5 was not detected in association with cell membranes, at first suggesting that it functioned in some aspect of the virus life cycle such as virion assembly or spread. Nevertheless, the I5L gene was readily deleted, and the mutant virus replicated and spread normally in a variety of host cells. This result was surprising because I5L is conserved in all chordopoxviruses, implying an important function. Thus, it was interesting to find that the deletion and frameshift mutants that did not express I5 were attenuated in a murine i.n. infection model. Thus, with an inoculum of 1×10^5 PFU (approximately five times the 50% lethal dose), there was a 90% survival rate. However, with a challenge dose 10 times higher, there were no survivors.

In anesthetized mice, the i.n. route results in primary infections in the upper and lower respiratory tracts, and the latter has been associated with morbidity and death (7, 10, 11, 13, 18). With a nonlethal dose of 10^4 PFU, on day 3 the lung titers of the I5L frameshift mutant and control VACV were similar, suggesting that the mutant virus was able to initially infect and replicate there. However, by day 7 the titer in mouse lungs of

the mutant was approximately 3 logs lower than the control, indicating less progression or more rapid clearance of the mutant. Examination of histological sections also indicated necrosis of the epithelium and underlying glandular tissue in the nasal passages of both the I5L mutant and the control virus at early times. However, there was less progression of the infection with the mutant virus than with the control virus and considerable recovery between days 7 and 10 relative to the control virus.

Our data suggest that I5 is involved in repelling the host antiviral defense though we cannot rule out some differences in cell tropism in vivo. Indeed, the latter would make sense in view of the location of I5 in the MV membrane. Further studies with a variety of primary mouse cells may help to evaluate this possibility. There have been a number of reports indicating that VACV triggers signaling pathways during the attachment or entry stage of infection (12, 14, 17), which could be mediated or partially suppressed by an MV membrane protein. Some information regarding these possibilities might be obtained in follow-up studies by analysis of inflammatory cells and cytokines in mouse lung washes as well as in vitro studies. The I5 protein is largely composed of two hydrophobic domains that presumably serve as transmembrane segments. There is a highly conserved 18-amino-acid sequence located between the two helices that could be an interaction domain for some cellular protein, and efforts to test this hypothesis are planned. A14.5, an even smaller conserved MV membrane protein of only 53 amino acids with a similar predicted topology, is also nonessential in cell culture but is required for virulence (1). It will be interesting to see if these two proteins have related roles.

ACKNOWLEDGMENTS

We thank Norman Cooper and Catherine Cotter for providing cells, Andrea S. Weisberg for electron microscopy, Lacey Cashell and Felix J. Santiago for mouse surgery, and Heather Hickman and Scott Hensley for advice on titration of virus from mouse lung tissue.

The work was supported by funds from the Division of Intramural Research, National Institute of Allergy and Infectious Diseases, National Institutes of Health.

REFERENCES

1. Betakova, T., E. J. Wolffe, and B. Moss. 2000. Vaccinia virus A14.5L gene encodes a hydrophobic 53-amino-acid virion membrane protein that enhances virulence in mice and is conserved amongst vertebrate poxviruses. *J. Virol.* **74**:4085–4092.
2. Chung, C. S., C. H. Chen, M. Y. Ho, C. Y. Huang, C. L. Liao, and W. Chang. 2006. Vaccinia virus proteome: identification of proteins in vaccinia virus intracellular mature virion particles. *J. Virol.* **80**:2127–2140.
3. Clamp, M., J. Cuff, S. M. Searle, and G. J. Barton. 2004. The Jalview Java alignment editor. *Bioinformatics* **20**:426–427.
4. Davies, D. H., L. S. Wyatt, F. K. Newman, P. L. Earl, S. Chun, J. E. Hernandez, D. M. Molina, S. Hirst, B. Moss, S. E. Frey, and P. L. Felgner. 2008. Antibody profiling by proteome microarray reveals the immunogenicity of the attenuated smallpox vaccine modified vaccinia virus Ankara is comparable to that of Dryvax. *J. Virol.* **82**:652–663.
5. Davison, A. J., and B. Moss. 1989. The structure of vaccinia virus late promoters. *J. Mol. Biol.* **210**:771–784.
6. Earl, P. L., N. Cooper, S. Wyatt, B. Moss, and M. W. Carroll. 1998. Preparation of cell cultures and vaccinia virus stocks, p. 16.16.1–16.16.3. In F. M. Ausubel, R. Brent, R. E. Kingston, D. D. Moore, J. G. Seidman, J. A. Smith, and K. Struhl (ed.), *Current protocols in molecular biology*, vol. 2. John Wiley and Sons, New York, NY.
7. Hayasaka, D., F. A. Ennis, and M. Terajima. 2007. Pathogeneses of respiratory infections with virulent and attenuated vaccinia viruses. *Virol. J.* **4**:22.
8. Katz, E., and B. Moss. 1970. Formation of a vaccinia virus structural polypeptide from a higher molecular weight precursor: inhibition by rifampicin. *Proc. Natl. Acad. Sci. USA* **6**:677–684.
9. Kyte, J., and R. F. Doolittle. 1982. A simple method for displaying the hydrophatic character of a protein. *J. Mol. Biol.* **157**:105–132.
10. Law, M., M. M. Putz, and G. L. Smith. 2005. An investigation of the therapeutic value of vaccinia-immune IgG in a mouse pneumonia model. *J. Gen. Virol.* **86**:991–1000.
11. Lee, S. L., J. M. Roos, L. C. McGuigan, K. A. Smith, N. Cormier, L. K. Cohen, B. E. Roberts, and L. G. Payne. 1992. Molecular attenuation of vaccinia virus: mutant generation and animal characterization. *J. Virol.* **66**:2617–2630.
12. Locker, J. K., A. Kuehn, S. Schleich, G. Rutter, H. Hohenberg, R. Wepf, and G. Griffiths. 2000. Entry of the two infectious forms of vaccinia virus at the plasma membrane is signaling-dependent for the IMV but not the EEV. *Mol. Biol. Cell* **11**:2497–2511.
13. Luker, K. E., M. Hutchens, T. Schultz, A. Pekosz, and G. D. Luker. 2005. Bioluminescence imaging of vaccinia virus: effects of interferon on viral replication and spread. *Virology* **341**:284–300.
14. Mercer, J., and A. Helenius. 2008. Vaccinia virus uses macropinocytosis and apoptotic mimicry to enter host cells. *Science* **320**:531–535.
15. Moss, B. 1996. Genetically engineered poxviruses for recombinant gene expression, vaccination, and safety. *Proc. Natl. Acad. Sci. USA* **93**:11341–11348.
16. Moss, B. 2007. *Poxviridae: the viruses and their replicaton*, p. 2905–2946. In D. M. Knipe, P. M. Howley, D. E. Griffin, R. A. Lamb, M. A. Martin, B. Roizman, and S. E. Straus (ed.), *Fields virology*, 5th ed., vol. 2. Lippincott Williams & Wilkins, Philadelphia, PA.
17. Rahbar, R., T. T. Murooka, A. A. Hinck, C. L. Galligan, A. Sassano, C. Yu, K. Srivastava, L. C. Platanias, and E. N. Fish. 2006. Vaccinia virus activation of CCR5 invokes tyrosine phosphorylation signaling events that support virus replication. *J. Virol.* **80**:7245–7259.
18. Reading, P. C., and G. L. Smith. 2003. A kinetic analysis of immune mediators in the lungs of mice infected with vaccinia virus and comparison with intradermal infection. *J. Gen. Virol.* **84**:1973–1983.
19. Resch, W., K. K. Hixson, R. J. Moore, M. S. Lipton, and B. Moss. 2007. Protein composition of the vaccinia virus mature virion. *Virology* **358**:233–247.
20. Szajner, P., A. S. Weisberg, J. Lebowitz, J. Heuser, and B. Moss. 2005. External scaffold of spherical immature poxvirus particles is made of protein trimers, forming a honeycomb lattice. *J. Cell Biol.* **170**:971–981.
21. Takahashi, T., M. Oie, and Y. Ichihashi. 1994. N-terminal amino acid sequences of vaccinia virus structural proteins. *Virology* **202**:844–852.
22. Trindade, G. S., G. L. Emerson, D. S. Carroll, E. G. Kroon, and I. K. Damon. 2007. Brazilian vaccinia viruses and their origins. *Emerg. Infect. Dis.* **13**:965–972.
23. Tulman, E. R., G. Delhon, C. L. Afonso, Z. Lu, L. Zsak, N. T. Sandybaev, U. Z. Kerembekova, V. L. Zaitsev, G. F. Kutish, and D. L. Rock. 2006. Genome of horsepox virus. *J. Virol.* **80**:9244–9258.
24. Turner, G. S. 1967. Respiratory infection of mice with vaccinia virus. *J. Gen. Virol.* **1**:399–402.
25. Upton, C., S. Slack, A. L. Hunter, A. Ehlers, and R. L. Roper. 2003. Poxvirus orthologous clusters: toward defining the minimum essential poxvirus genome. *J. Virol.* **77**:7590–7600.
26. Yoder, J. D., T. S. Chen, C. R. Gagnier, S. Vemulapalli, C. S. Maier, and D. E. Hruby. 2006. Pox proteomics: mass spectrometry analysis and identification of vaccinia virion proteins. *Virol. J.* **3**:10.